Sb- and Al- Free Ultra-High-Current Tunnel FET Designs

Jun Z. Huang[1], Pengyu Long[1], Michael Povolotskyi[2], Gerhard Klimeck[1], Mark J.W. Rodwell[3]
[1]Network for computational nanotechnology, Purdue University, West Lafayette, IN 47907
[2]Discovery Park, Purdue University, West Lafayette, IN 47907
[3]ECE Department, University of California, Santa Barbara, CA 93106
Email: junhuang1021@gmail.com

Abstract We propose a series of ultra-high-current triple-heterojunction (3HJ) tunnel field-effect transistor (TFET) designs based on InGaAs/InP materials. Such materials are Sb- and Al- free for ease of processing and to permit low-trap-density dielectric interfaces. Quantum transport simulations, based on eight-band $k \cdot p$ Hamiltonian, considering effects of strain and electron-phonon scattering, are performed to guide the design and predict the device performance. With V_{DD}=0.3V and I_{OFF}=1nA/μm, the best design can achieve ballistic I_{ON} of 605μA/μm and, with electron-phonon scattering modeled at 310eV/nm optical deformation constant, a still-high 392μA/μm.

Introduction Heterojunction (HJ) designs have been widely incorporated to improve the tunneling probability of TFETs [1]. 3HJ designs, recently reported in [2]-[4], further improve the tunneling probability, leading to extremely high ON current in simulations. Those 3HJ designs, however, were based on either Sb- or Al-containing materials to which no low-trap-density dielectric interfaces have been reported. Although an InP-based design has been proposed to avoid use of Al-containing materials [5], the presence of Sb-containing materials, such as GaSb and GaAsSb, still introduces difficulties in processing due to the tendency of GaSb to inadvertently etch in photoresist developer. HJ TFETs, unlike many other HJ devices, present a particular challenge in fabrication, because the TFET PN junction and heterointerfaces must be perpendicular to the dielectric-semiconductor interface. One way to address this challenge is to grow vertical nanowire structures [6], but a challenge here is to scale the nanowire diameter from the present ~20nm to smaller dimensions as high-density integration is sought. Another method to form TFETs is to form lateral nanosheet or nanowire devices using Template Assisted Selective Epitaxy, also known as confined epitaxial lateral overgrowth [7]. For the 2nd approach, a particular difficulty with InAs/GaSb-based TFET designs is the potential of Sb-containing materials to show parasitic growth nucleation on the dielectric surfaces of the growth template. This study proposes a series of 3HJ TFET designs based entirely on InGaAs/InP materials. Simulations show that these Sb- and Al- free designs also have very high ON currents, comparable to previous designs [3]-[5].

Proposed Designs As shown in Fig. 1, the device is based on a double-gate ultra-thin-body (UTB) structure. The designs consist of an InP source (p-type doped), an $In_xGa_{1-x}As$ source well (p-type doped), an $In_yGa_{1-y}As$ channel well (intrinsic), an InP channel (intrinsic), and an InP drain (n-type doped). To have a small tunnel barrier height and a large electric field at the tunnel junction, the source well should have a large valence band offset (VBO) relative to the InP source, while the channel well should have a large conduction band offset (CBO) relative to the InP channel. Moreover, to facilitate tunneling, the source well should have a small hole effective mass while the channel well should have a small electron effective mass. Therefore, three designs have been considered, as shown in Table 1: (1) x=0.53, y=0.53; (2) x=0.26, y=0.77; and (3) x=0, y=1. The design (1) comprises of only two HJs instead of three, and the quantum well layers are lattice matched to InP layers. In the design (2), if the quantum well layers are strained to match the surrounding InP layers, the source (channel) well will have 1.91% (1.62%) tensile (compressive) strain in the plane perpendicular to the transport direction. In design (3), the source (channel) well will have 3.81% (3.13%) tensile (compressive) strain. Fig. 2 shows the band diagrams of the six materials considered above, with the band properties summarized in Table 2. They are calculated using the eight-band $k \cdot p$ method including strain [8]. The room-temperature parameters of the binaries are taken from [9]. For the alloys, the parameters are obtained from linear interpolation considering bowing (where applicable). It is found that the GaAs with compressive strain has the largest VBO relative to the InP source and a very small hole effective mass; the InAs with tensile strain has the largest CBO relative to the InP channel and a slightly larger electron effective mass. These materials are chosen for design (3). Since design (3) has a large amount of strain, to reduce the strain we can use a Ga-rich material, $Ga_{0.74}In_{0.26}As$, for the source well and an In-rich material, $Ga_{0.23}In_{0.77}As$, for the channel well, which leads to the

design (2). As shown in Table 2, the VBO and CBO of these two materials (with strain) are less than those of design (3), but still sufficient for good TFET performance. The design (1) is the special case of zero strain, and with the smallest CBO and VBO. In this work, the gate oxide has thickness T_{ox}=1.8nm and dielectric constant $\varepsilon_{r,ox}$=9.0. The p-type doping density is 5×10^{19}/cm^3 and the n-type doping density is 2×10^{19}/cm^3. The UTBs are confined in the [1-10] crystal direction and the transport is along the [110] direction. The channel thickness T_{ch} and the channel length L_g are set to be 4.0nm and 30nm, respectively. The quantum well lengths L_{sw} and L_{cw} are then optimized to maximize the ON current, resulting in (1) L_{sw}=4.0nm, L_{cw}=4.5nm; (2) L_{sw}=L_{cw}=4.0nm; and (3) L_{sw}=4.0nm, L_{cw}=3.5nm.

Simulation Method and Results The quantum transmitting boundary method is used for ballistic transport simulation [10], while non-equilibrium Green's function method in the self-consistent Born approximation is used to study the electron-phonon (acoustic and optical) scattering effect [11]. To reduce the computational cost, we consider only diagonal components in the scattering self-energy and adjust the optical deformation constant to fit to bulk carrier mobility [4] [5]. Fig. 3 compares the band diagrams and transmissions of the three designs at the ON state. It is found that design (3) has the smallest tunnel barrier height and shortest tunnel distance, which lead to the largest transmission, followed by design (2) and (1). Fig. 4 shows that two resonances are created in the quantum well regions, further enhancing the transmission at the ON state, but will also lead to stronger phonon-assisted tunneling leakage at the OFF state. Fig. 5 compares the transfer characteristics of the three designs. It shows that design (3) has the largest ON current, followed by design (2) and (1). Electron-phonon scattering, modeled at 310eV/nm optical deformation constant (leading to mobility μ_n(InAs)=1.35×10^4cm^{2}V^{-1}s^{-1}), somewhat degrades the subthreshold swing hence ON current, but the ON currents are still very high especially for design (3) and (2).

Conclusion The performance of the proposed three designs is summarized in Table 3, indicating that a series of high-current 3HJ TFET designs are obtained. These designs are based entirely on common InGaAs/InP materials and different layers are strain-compensated, making them promising options for future experimental study.

Acknowledgment:

This work was supported in part by the nanoHUB.org computational resources operated by the Network for Computational Nanotechnology funded by the U.S. National Science Foundation under Grant EEC-0228390, Grant EEC-1227110, Grant EEC-0634750, Grant OCI-0438246, Grant OCI-0832623, and Grant OCI-0721680, in part by the National Science Foundation under Award 1509394 and Award 1639958, and in part by the Semiconductor Research Corporation under Award 2694.03.

References:

[1] A. M. Ionescu and H. Riel, "Tunnel field-effect transistors as energy-efficient electronic switches," *Nature*, vol. 479, p. 329, Nov. 2011. [2] P. Long *et al.*, "Extremely high simulated ballistic currents in triple-heterojunction tunnel transistors," in *Proc. 74th Annu. Device Res. Conf. (DRC)*, Jun. 2016, p. 1. [3] J. Z. Huang *et al.*, "P-type tunnel FETs with triple heterojunctions," *IEEE J. Electron Devices Soc.*, vol. 4, p. 410, Nov. 2016. [4] P. Long *et al.*, "A tunnel FET design for high-current, 120 mV operation," in *IEDM Tech. Dig.*, Dec. 2016, p. 30.2.1. [5] P. Long *et al.*, "A high-current InP-channel triple heterojunction tunnel transistor design," in *Proc. 75th Annu. Device Res. Conf. (DRC)*, Jun. 2017, p. 1. [6] E. Memisevic *et al.*, "Vertical InAs/GaAsSb/GaSb tunneling field-effect transistor on Si with S = 48 mV/decade and Ion = 10 μA/μm for Ioff = 1 nA/μm at Vds = 0.3 V," in *IEDM Tech. Dig.,* Dec. 2016, p. 19.1.1. [7] D. Cutaia *et al.*, "Complementary III–V heterojunction lateral NW Tunnel FET technology on Si," in *IEEE Symposium on VLSI Technology*, Jun. 2016, p. 1. [8] T. B. Bahder, "Eight-band k.p model of strained zinc-blende crystals," *Phys. Rev. B*, vol. 41, p. 11992, 1990. [9] I. Vurgaftman *et al.*, "Band parameters for III–V compound semiconductors and their alloys," *J. Appl. Phys.*, vol. 89, p. 5815, 2001. [10] S. Steiger *et al.*, "NEMO5: A parallel multiscale nanoelectronics modeling tool," *IEEE Trans. Nanotechnol.*, vol. 10, p. 1464, Nov. 2011. [11] J. Charles *et al.*, "Incoherent transport in NEMO5: realistic and efficient scattering on phonons," *J. Comput. Electron.*, vol. 15, p. 1123, 2016.

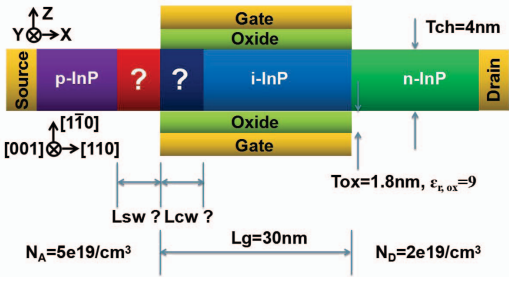

Figure 1. Device structure, material composition, and design parameters of the 3HJ TFET designs.

Design	Source well	Channel well
(1) Lattice-matched	p-$Ga_{0.47}In_{0.53}As$ (unstrained)	i-$Ga_{0.47}In_{0.53}As$ (unstrained)
(2) Lightly-strained	p-$Ga_{0.74}In_{0.26}As$ (1.91% tensile strain)	i-$Ga_{0.23}In_{0.77}As$ (1.62% compressive strain)
(3) Heavily-strained	p-GaAs (3.81% tensile strain)	i-InAs (3.13% compressive strain)

Table 1. Material compositions for the quantum wells of the proposed three designs. Note: both the source and channel wells are assumed to be strained to match the lattice constant of InP.

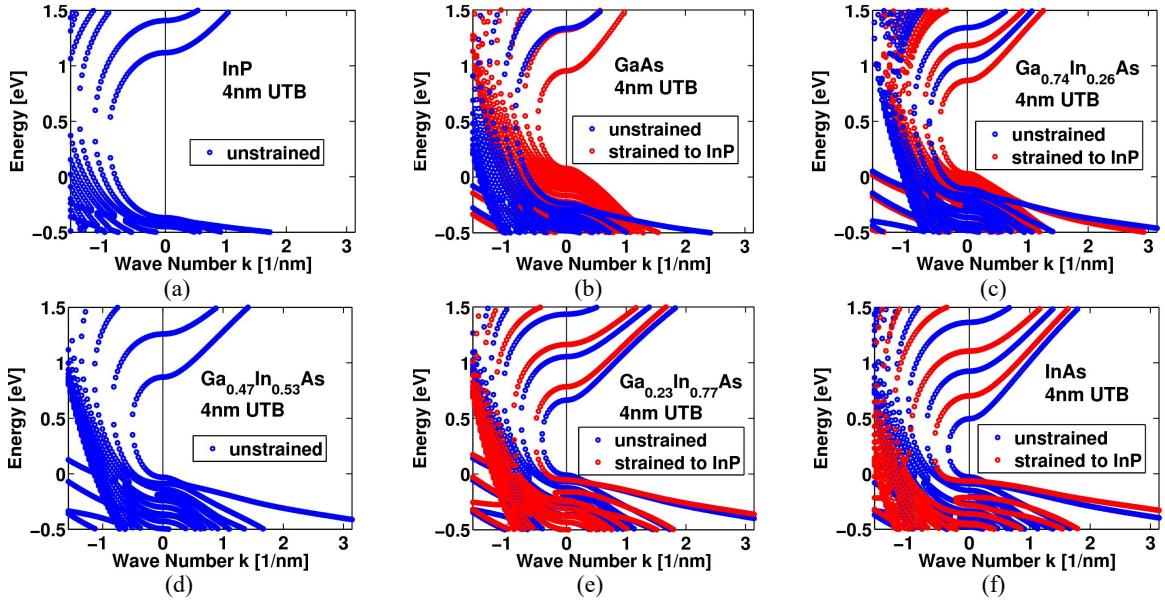

Figure 2. Complex and real band structures (at k_y=0) of the the six UTBs considered in this study. Tensile (compressive) strain decreases (increases) the band gap and effective masses.

Material (UTB)	Band gap (eV)	VBO (eV)	CBO (eV)	Electron effective mass (m_0)	Hole effective mass (m_0)
InP	1.4884	0	0	0.0940	0.1306
Tensile strained GaAs	0.8762	0.4466	-0.1656	0.0416	0.0428
Tensile strained $Ga_{0.74}In_{0.26}As$	0.8412	0.3962	-0.2510	0.0439	0.0413
$Ga_{0.47}In_{0.53}As$	0.9034	0.3370	-0.2480	0.0534	0.0560
Compressive strained $Ga_{0.23}In_{0.77}As$	0.8365	0.3169	-0.3350	0.0570	0.1332
Compressive strained InAs	0.7675	0.3036	-0.4173	0.0595	0.2893

Table 2. Summary of band offsets (relative to InP) and effective masses of the six UTBs considered in this study.

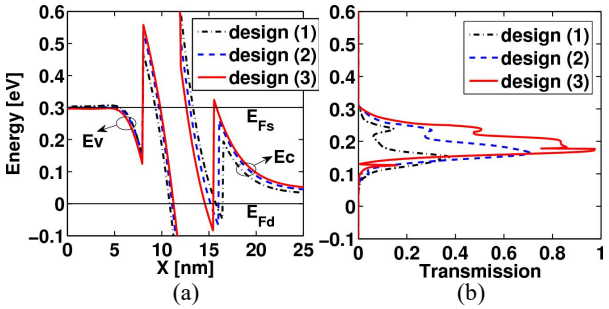

Figure 3. Band diagram (a) and transmission (b) at ON state for the three designs. Source (drain) Fermi level is E_{Fs} (E_{Fd}).

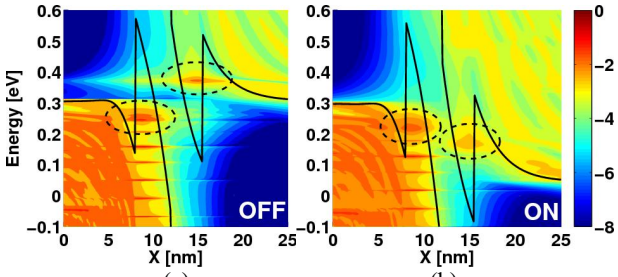

Figure 4. Ballistic local density of states (LDOS) of design (3) at OFF state (a) and ON state (b), respectively.

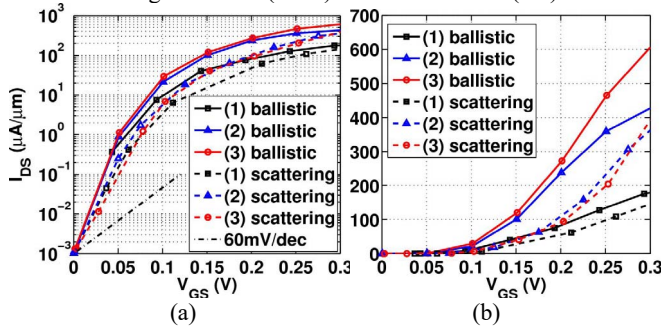

Figure 5. Log scale (a) and linear scale (b) transfer characteristics (ballistic and with electron-phonon scattering) at V_{DS}=0.3V for the three designs. All *I-V* curves are shifted to the same I_{OFF}=1nA/μm at V_{GS}=0V.

Design	Ballistic		Scattering	
	SS	I_{ON}	SS	I_{ON}
(1) Lattice-matched	14.8	179	20.1	144
(2) Lightly-strained	14.0	427	26.3	358
(3) Heavily-strained	13.8	605	33.5	392

Table 3. Subthreshold swing (SS) at V_{GS}=0, and ON current (I_{ON}) at V_{DD}=0.3V and I_{OFF}=1nA/μm, for the three designs. The unit of SS is mV/dec and the unit of I_{ON} is μA/μm.